ACS OMEGA

http://pubs.acs.org/journal/acsodf

Article

Silymarin-Functionalized Selenium Nanoparticles Prevent LPS-Induced Inflammatory Response in RAW264.7 Cells through Downregulation of the PI3K/Akt/NF-κB Pathway

Xiao-jie Mi,[§] Ha-Minh Le,[§] Sanghyun Lee, Hye-Ryung Park, and Yeon-Ju Kim*

Cite This: *ACS Omega* 2022, 7, 42723−42732

Read Online

ACCESS | Metrics & More | Article Recommendations

ABSTRACT: Silymarin exhibits an anti-inflammatory property in various cancers and inflammatory diseases. In our previous work, silymarin-mediated selenium nanoparticles (SeNPs) (Si-SeNPs) were developed using a green synthesis technique, and its potential as an anticancer agent was confirmed. In order to further examine the extended comprehensive potential of Si-SeNPs, this investigation focuses on studying the enhanced anti-inflammatory effect of Si-SeNPs in lipopolysaccharide (LPS)-stimulated RAW264.7 macrophages. Enzyme-linked immunosorbent assay and quantitative reverse transcription-polymerase chain reaction were used to evaluate the expression of pro-inflammatory mediators and cytokines. Western blotting and immunofluorescence assays were conducted to assess the protein expression of p-PI3K, p-Akt, p-NF-κB, and p-IκBα. Compared to silymarin, Si-SeNPs exhibited a significantly increased inhibitory effect on LPS-induced release of nitric oxide and the expression of pro-inflammatory cytokines such as tumor necrosis factor-alpha (TNF-α) and interleukin 1β (IL-1β) in RAW264.7 cells. A western blot assay indicated that Si-SeNPs downregulated the PI3K/Akt and NF-κB signaling pathways. The immunofluorescence assay suggested that Si-SeNPs inhibited the nuclear translocation and the activation of NF-κB. In addition, 740 Y−P (PI3K agonist) was used to demonstrate that activating the PI3K/Akt signal could partially reverse the inflammatory response, suggesting a causal role of the PI3K/Akt signaling pathway in the anti-inflammatory effect of Si-SeNPs. Consequently, these findings indicate that Si-SeNPs could be a functional agent of the attenuation of LPS-induced inflammatory responses in RAW264.7 macrophages through inhibiting the PI3K/Akt/NF-κB signaling pathway. In addition, biosynthesized Si-SeNPs could be more effective at reducing inflammation than only silymarin extracts. Thus, this study lays an experimental foundation for the clinical application of using biosynthesized SeNPs as a novel candidate in the field of inflammation-associated diseases.

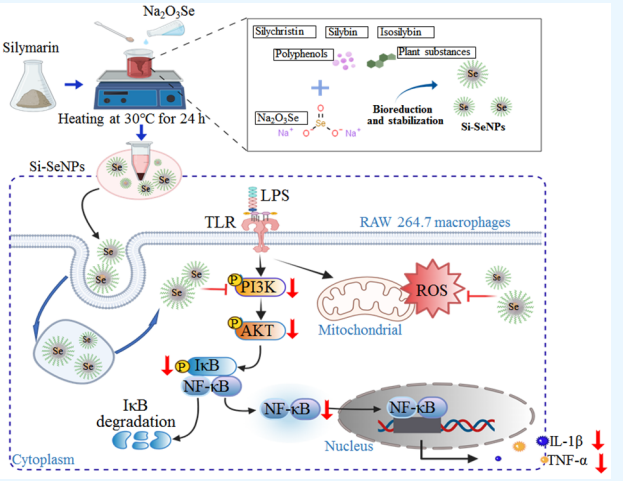

1. INTRODUCTION

Inflammation is a natural protective immune response to hazardous stimuli, such as microbial pathogen infection, tissue injury, or toxic compounds.[1] Excessive and prolonged inflammatory responses can lead to many progressive and chronic diseases such as cancer, Parkinson's disease, and autoimmune conditions.[2] Macrophages, which belong in the principal defense mechanism, are of essential importance in innate immunity.[3] Lipopolysaccharide (LPS), the primary component within the cell membrane of gram-negative bacteria, can stimulate macrophages to secrete large amounts of inflammatory cytokines and mediators, including IL-1β, TNF-α, and nitric oxide.[4] Therefore, inhibition of production of these mediators and cytokines is a promising idea for the design of anti-inflammatory drugs.[5] There is a wide range of available anti-inflammatory medicines; however, their applications are still associated with many side effects such as increased risk of cardiovascular disease, kidney disease, or gastrointestinal ulcers.[6] Recently, as an alternative approach for the treatment of inflammation, nano-biotechnology has attracted much attention.

Silymarin, a phytochemical substance extracted from the herbal medicine *Silybum marianum* L., is illustrious because of its anti-inflammatory and antioxidant activities. However, due to its poor water and liquid solubility as well as low gut absorption

Received: July 1, 2022
Accepted: October 17, 2022
Published: November 16, 2022

(20%−50%), silymarin shows low bioavailability and limits clinical application.[7] As is well-known, silymarin is composed of seven major flavonolignans (silydianin, silychristin, isosilybin A, isosilybin B, isosilychristin, silybin A, silybin B).[8,9] The high flavonolignans content and anti-inflammatory property of silymarin make it a valuable source of bioactive compounds acting as the reducing and capping agent in the green synthesis of nanoparticles.[10]

The evolution of nanotechnology has advanced biomedicine therapeutics through innovative approaches to drug delivery and disease treatment.[11] Selenium nanoparticles (SeNPs) have been employed widely in research ranging from anti-inflammation to anticancer treatments due to their benefits of low toxicity, high stability, and biocompatibility.[12,13] To encourage the biomedical applications of SeNPs, biosynthesis methods have been promoted to use to produce less toxic and highly bioactive SeNPs. Nonetheless, biosynthesis methods using fungi, bacteria, or algae have several disadvantages including time-consuming production methods and difficulty in controlling size and morphology.[14] Therefore, phytochemicals from plant extracts have been applied as alternatives to microbial-mediated biosynthesis of SeNPs.[15] In a previous study, we successfully synthesized silymarin-mediated SeNPs (Si-SeNPs) with mixed shapes and sizes in the range of 30−80 nm, and we confirmed 31.1% of silymarin was coated on the surface of SeNPs. The enhanced anticancer efficacy of Si-SeNPs compared to silymarin has been demonstrated in various cancer cells such as HeLa, AGS, HepG2, and A549 cells.[8] Long-term chronic inflammation promotes cancer progression in the body, and 15%−20% of cancer deaths globally are related to inflammatory events.[16] Associated with the evidence of silymarin's anti-inflammatory effects in a range of malignancies and inflammatory diseases,[17] we hypothesized that biosynthesized Si-SeNPs could exert better anti-inflammatory activities than only silymarin extracts. In the present study, we further explored the anti-inflammatory efficacy of Si-SeNPs in RAW264.7 macrophages and investigated the underlying molecular mechanisms to examine the extended comprehensive potential of Si-SeNPs.

2. MATERIALS AND METHODS

2.1. Reagents and Antibodies. RAW264.7 cells were obtained from the Korean Cell Line Bank. Dulbecco's Modified Eagle Medium (DMEM), penicillin-streptomycin, and fetal bovine serum (FBS) were obtained from GenDEPOT. Silymarin, dimethyl sulfoxide (DMSO), soluble 3-(4, 5-dimethylthiazol-2-yl)-2, 5-diphenyltetrazolium bromide (MTT), sodium selenite, and lipopolysaccharide (LPS) were purchased from Sigma-Aldrich. Sodium selenite was purchased from Sigma Chemicals Co. The 740Y−P was purchased from MedChemExpress (MCE). Primary antibodies against PI3K, p-PI3K, AKT, and p-AKT were obtained from Abcam, and antibodies against IκBα, p-IκBα, NF-κB, p-NF-κB, and β-actin were purchased from Cell Signaling Technology.

2.2. Biosynthesis and Physicochemical Characterization of Si-SeNPs. The synthesis of Si-SeNPs followed our previous publication.[8] A mixture of sodium selenite (Na_2SeO_3) and silymarin solutions was magnetically stirred in the dark at 30 °C for 24 h. After the successful synthesis of Si-SeNPs, field emission transmission electron microscopy (TEM; JEM-2100F, JEOL, Ltd.) was used to estimate the size and morphology of the Si-SeNPs at 200 kV. The size, dispersal nature, and zeta potential of Si-SeNPs were determined by a Dynamic Light Scattering (DLS) particle analyzer (Otsuka Electronics) at 25 °C.

2.3. Cell Culture and Cell Viability Assay. The RAW264.7 macrophage cells were grown in DMEM supplemented with 10% heat-inactivated FBS and 1% penicillin−streptomycin at 37 °C in a 5% CO_2 humidified incubator. The MTT assay was used to analyze the cytotoxicity of silymarin and Si-SeNPs against RAW264.7 cells. The cells were seeded (1×10^4 cells/well) in a 96-well culture plate and incubated for 24 h. When the confluence reached 90%, cells were treated with two concentrations each of Silymarin and Si-SeNPs (0.4 and 0.8 μg/mL). After 24 h, 100 μL of MTT (0.5 mg/mL) was added into each well to further incubate for 3 h, and then the medium was replaced with DMSO to dissolve the dark formazan. Absorbance was measured at 570 nm using a microplate reader (SpectraMax ABS Plus).

2.4. Nitric Oxide Analysis. RAW264.7 cells were separately plated in 96-well plates (1×10^4 cells/well) for 24 h and pretreated with Si-SeNPs and silymarin (0.4, 0.8 μg/mL) for 1 h, then stimulated with LPS (1 μg/mL) for another 24 h. The cell morphology in each group was observed using phase microscopy. The production of nitrite ($NaNO_2$) and nitric oxide (NO) oxidation was determined using the Griess Reagent (Thermo Fisher Scientific) according to the manufacturer's protocol. After this was incubated for 30 min at 25 °C, the absorbance of $NaNO_2$ and MTT was measured at 570 nm using a spectrophotometric microplate reader.

2.5. Reactive Oxygen Species and Mitochondrial Superoxide Detection. Cells treated with silymarin or Si-SeNPs (0.4 and 0.8 μg/mL) for 24 h were incubated with the oxidative stress and superoxide detection reagent at 37 °C for 30 min. Intracellular reactive oxygen species (ROS) were released, and mitochondrial superoxide (Mito-SOX) was detected using the Cellular ROS/(Mito-SOX) Detection Assay Kit (Abcam) containing the oxidative stress (green) and superoxide detection reagent (orange). Fluorescence was measured using LSM 510 and 510 META laser scanning microscopes (Leica).

2.6. Live/Dead Cell Fluorescence Staining. After cell treatment, the live/dead viability staining kit (Life Technologies) was used to evaluate the cytotoxicity effect of samples according to the manufacturer's instructions. The living cells (green) and dead cells (red) were visualized using a fluorescence microscope (Leica).

2.7. Enzyme Immunosorbent Assay (ELISA). The secretion levels of mouse TNF-α and IL-1β were estimated using an enzyme-linked immunosorbent assay (ELISA) kit (R&D Systems) following to the manufacturer's instruction. RAW 264.7 macrophages (1×10^4 cells/well) were seeded into 96-well plates and treated with silymarin and Si-SeNPs, followed by stimulation with 1 μg/mL LPS for 24 h. After that, supernatants were collected to determine the level of these cytokines.

2.8. Immunofluorescence Staining. After 24 h of treatment with silymarin and Si-SeNPs, the cells were fixed in 4% paraformaldehyde for 30 min and permeabilized with 1% Triton X-100 in phosphate-buffered saline (PBS). Then, the cells were blocked with 5% bovine serum albumin (BSA) for 1 h before incubation with the primary antibody (1:1000) overnight at 4 °C. After three washes with PBS, the cells were incubated with Alexa Fluor 488-conjugated goat antirabbit IgG and Alexa Fluor 594-conjugated goat antirabbit IgG H&L (Abcam) for 1 h in the dark. The nuclei were counterstained with 4′,6-diamidino-2-phenylindole (DAPI). Immunofluorescence was captured using a fluorescence microscope (Leica).

https://doi.org/10.1021/acsomega.2c04140
ACS Omega 2022, 7, 42723−42732

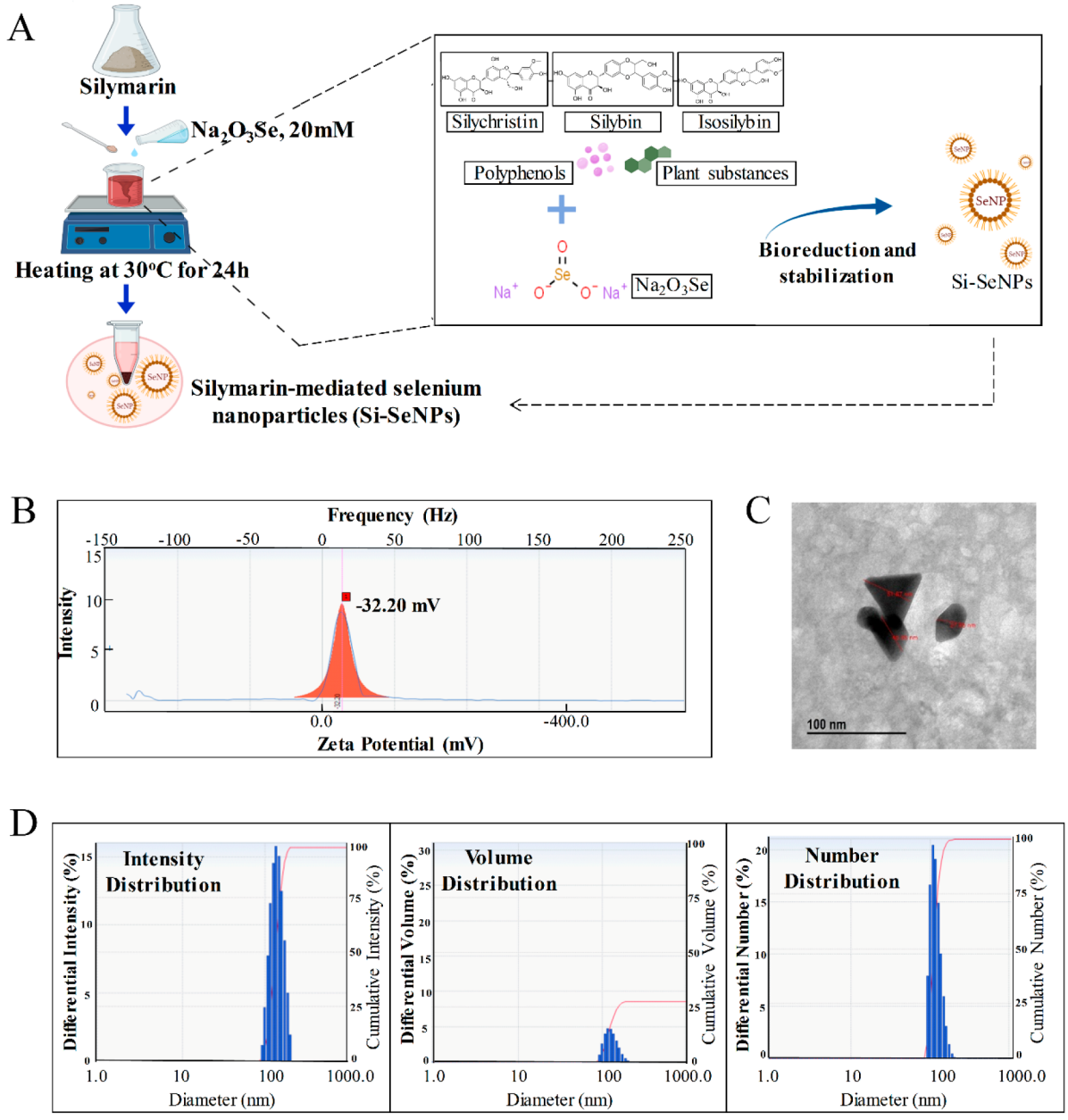

Figure 1. Biosynthesis and characterization of Si-SeNPs. Biosynthesis of Si-SeNPs (A). Zeta potential of Si-SeNPs (B). Field emission TEM images of Si-SeNPs (C). DLS spectrum of Si-SeNPs (D).

2.9. Quantitative Real-Time PCR (qRT-PCR). Total RNA was extracted from RAW264.7 cells using the Trizol reagent kit protocol (Bioline, Brisbane, Australia). Total RNA (500 ng) was reverse transcribed into cDNA using a Superscript First-Strand Synthesis Kit (Invitrogen). Quantitative reverse transcription-polymerase chain reaction (qRT-PCR) was performed according to the manufacturer's instructions using the SYBR Premix Ex *Taq*II RT-PCR Kit (TaKaRa Bio Inc.). The cDNA was amplified by qRT-PCR using specific primers for *IL-1β*: forward 5′-TGCAGAGTTCCCCAACTGGTAC-3′ and reverse 5′-GTGCTGCCTAATGTCCCCTTGAATC-3′; *TNF-α*: forward 5′-AGCCCACGTCGTAGCAAACCAC-3′ and reverse 5′-AACACCCATTCCCTTCACAGAGC-3′; *GAPDH*: forward 5′-ACCACAGTCCATGCCATCAC-3′ and reverse 5′-CCACCACCCTGTTGCTGTAG-3′. Each sample was analyzed in triplicate. GAPDH was used as an internal control to evaluate the relative gene expression.

2.10. Western Blot Analysis. Total cellular protein was extracted using a radioimmunoprecipitation assay (RIPA) lysis buffer (Thermo Fisher Scientific). RIPA lysis buffer was added to the cells on ice for 1 h, and the lysates were centrifuged at 4 °C for 20 min. A Bio-Rad Protein Assay Kit (Bio-Rad Laboratories Inc.) was used to analyze the protein concentration; proteins (40 μg) were loaded on a 10% sodium dodecyl sulfate-polyacrylamide gel (SDS-PAGE) and then transferred to poly(vinylidene difluoride) (PVDF) membranes (Thermo Fisher Scientific). The membranes were blocked with 5% skim milk at room temperature for 1 h and immunoblotted overnight at 4 °C with primary antibodies (1:1000 dilution), using β-actin as an internal control. After three washes with phosphate-buffered saline with Tween (PBST), the membranes were

https://doi.org/10.1021/acsomega.2c04140
ACS Omega 2022, 7, 42723−42732

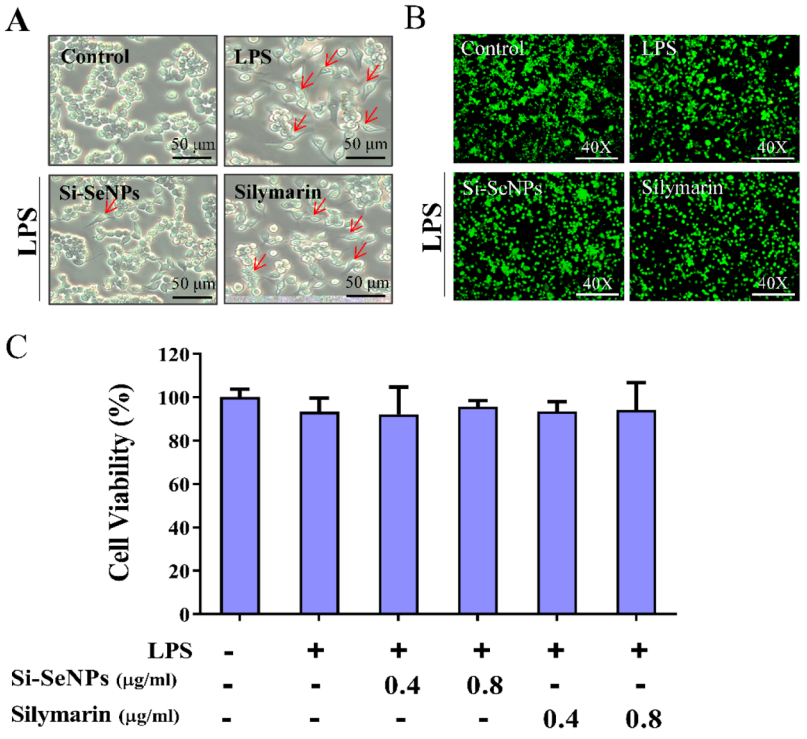

Figure 2. Si-SeNPs alleviate LPS-induced RAW264.7 cell differentiation. The effect of Si-SeNPs and silymarin on the cellular morphology of LPS-activated RAW264.7 cells (A). The effect of Si-SeNPs and silymarin on the viability of RAW264.7 cells using live/dead staining, with green color (live cells) and red color (dead cells) (B). The effect of Si-SeNPs and silymarin on the viability of RAW264.7 cells using MTT assay (C).

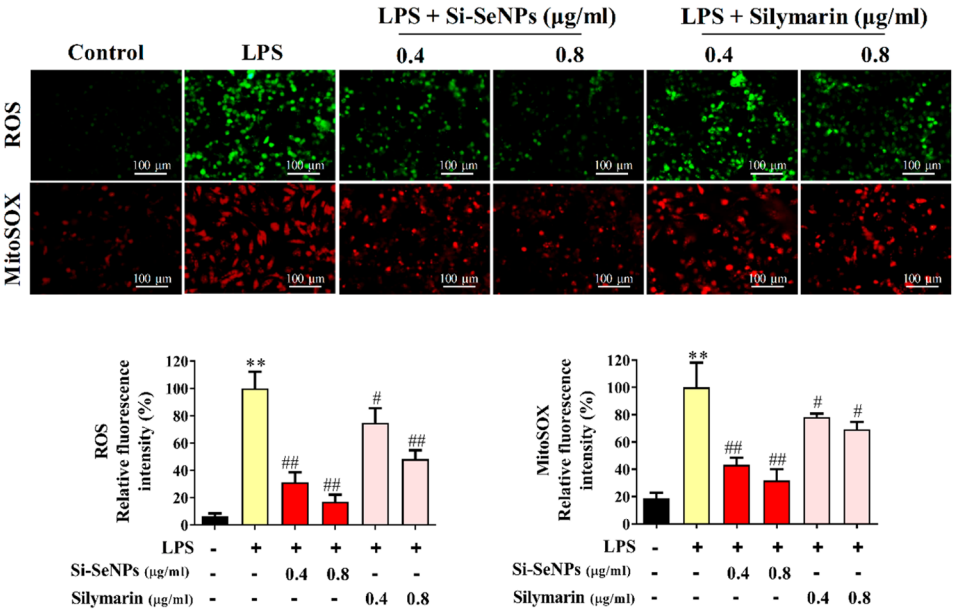

Figure 3. Effect of Si-SeNPs on ROS (green) and MitoSOX (red) generations in LPS-stimulated RAW264.7 cells. All values are expressed as mean ± SD. (**) $p < 0.01$ vs control group; (#) $p < 0.05$, (##) $p < 0.01$ vs LPS group.

incubated with the appropriate horseradish peroxidase (HRP)-conjugated secondary antibody (1:5000 dilution) for 1 h in a dark box. Protein bands were visualized with the West-Q Pico ECL Solution (GenDEPOT) and quantified using the Image-J software.

2.11. Statistical Analysis. The mean ± standard deviation (SD) of three independent experiments was performed in this study. Statistical analyses were employed by GraphPad Prism 8 (GraphPad Software, Inc.). Statistical comparisons between groups were assessed by a Student's *t*-test with the significant consideration at $p < 0.05$ and $p < 0.01$.

3. RESULTS

3.1. Biosynthesis and Characterization of Si-SeNPs. Based on our previous research, synthesized Si-SeNPs followed a redox reaction in which the biological molecules of silymarin

https://doi.org/10.1021/acsomega.2c04140
ACS Omega 2022, 7, 42723−42732

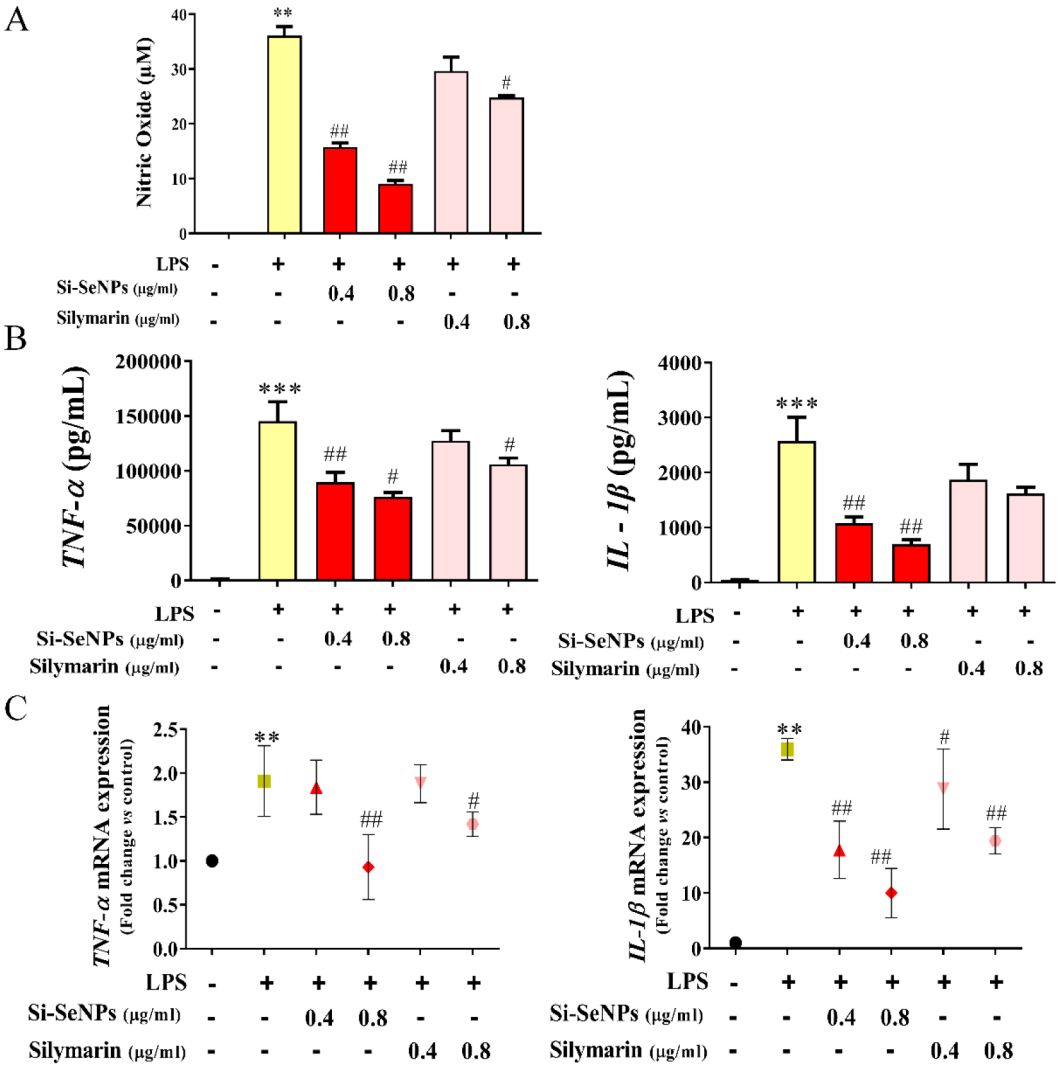

Figure 4. Inhibitory effect of Si-SeNPs on inflammation end product in LPS-stimulated RAW264.7 cells. The inhibitory effect of Si-SeNPs and silymarin on NO production in LPS-treated RAW264.7 macrophages (A). Secretion of TNF-α and IL-1β measured in the cell supernatant using ELISA kits (B). Analysis of gene expression (*TNF-α* and *IL-1β*) after Si-SeNPs or silymarin treated in activated macrophages (C). All values are expressed as mean ± SD. (**) $p < 0.01$ vs control group; (#) $p < 0.05$, (##) $p < 0.01$ vs LPS group.

along with sodium selenite functioned as reducing and stabilizing agents (Figure 1A). The Si-SeNPs contain three main flavonolignan compounds (silychristin, silybin, and isosilybin), and it was confirmed that an organic polymer coating emerged on the Si-SeNPs surface. To test the stability of Si-SeNPs, the zeta potential was measured at −32.2 mV, which was considered stable (Figure 1B). In a TEM image, the Si-SeNPs possessed sizes that ranged from approximately 30 to 80 nm and were in the form of spherical-, triangular-, and hexagonal-shaped mixed nanohybrids (Figure 1C). The hydrodynamic size of the Si-SeNPs was measured by DLS technique to be around 192.1 nm. The polydispersity index was 0.1, indicating the narrow size distribution of SeNPs.

3.2. The Effect of Si-SeNPs on Lipopolysaccharide (LPS)-Induced RAW264.7 Cell Differentiation. To study the protective effects of Si-SeNPs on LPS-stimulated RAW264.7 cells, the morphological changes induced by a Si-SeNPs treatment were first investigated in LPS-treated cells through optical microscopy. As shown in Figure 2A, the RAW264.7 cells had a round shape with smooth edges and without pseudopodia. However, LPS-induced abundant cell differentiation (red arrow) showed cell morphological variations that were flat and elongated in shape with pseudopodia formation. Following Si-SeNPs (0.8 μg/mL) treatment, the cell morphological structure was changed to be ameliorated. Following a Si-SeNPs (0.8 μg/mL) treatment, the cell morphological structure was changed to be ameliorated. To examine the cytotoxic impacts of Si-SeNPs on LPS-stimulated RAW264.7 cells, live/dead staining was evaluated initially, and no toxicity was observed in all groups. In an MTT assay, cells were pretreated with Si-SeNPs and silymarin (0.4 and 0.8 μg/mL). As shown in Figure 2B, there were no considerable cytotoxic effects under the Si-SeNPs and silymarin (0.4 and 0.8 μg/mL) treatment conditions through the MTT assay.

3.3. The Effect of Si-SeNPs on ROS Production in LPS-Induced RAW264.7 Macrophages. ROS production is responsible for macrophage differentiation and plays a critical role in the activation of key inflammatory signaling pathways.[18] In this study, we assessed the ability of Si-SeNPs and the extract of silymarin to influence the level of ROS and MitoSOX in RAW264.7 cells stimulated by LPS. In comparison to the control group, LPS substantially increased the fluorescence

https://doi.org/10.1021/acsomega.2c04140
ACS Omega 2022, 7, 42723−42732

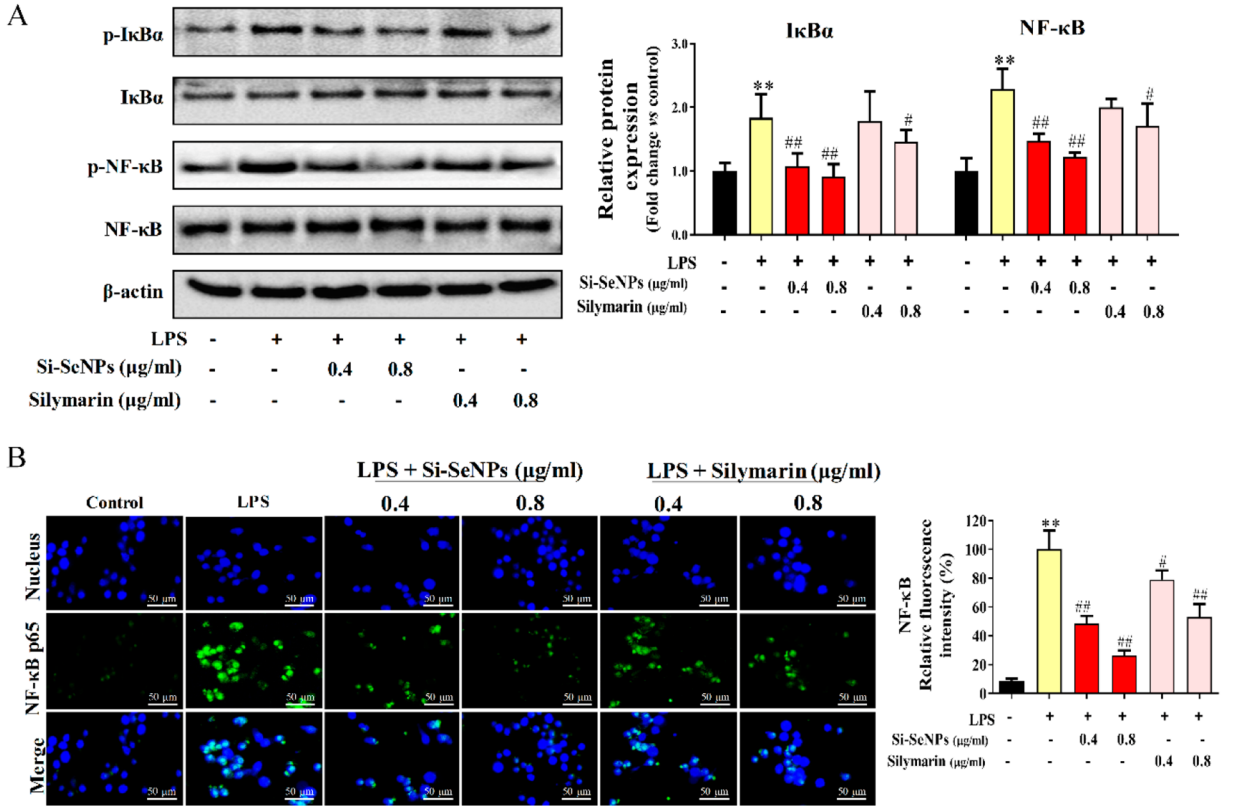

Figure 5. Inhibitory effect of Si-SeNPs and silymarin on NF-κB signaling pathway. For NF-κB protein expression, RAW264.7 cells were treated with Si-SeNPs and silymarin (0.4 and 0.8 μg/mL) and exposed to LPS (1 μg/mL) for 24 h (A). p65 translocation was established using an NF-κB antibody and an Alexa Fluor 488-conjugated goat antirabbit IgG and 594-conjugated goat antirabbit IgG H&L. Nuclei were countered by DAPI. Scale bar = 50 μm (B). All values are expressed as mean ± SD. (**) $p < 0.01$ vs control group; (#) $p < 0.05$, (##) $p < 0.01$ vs LPS group.

intensity with ROS (green) and MitoSOX (red), whereas, at the concentration 0.8 μg/mL, Si-SeNPs pretreated cells significantly reduced the fluorescence intensity to 16.7% and 31.8%, respectively. In addition, compared to Si-SeNPs, 0.8 μg/mL silymarin decreased ROS production and MitoSOX expression to 48.2% and 69.3%, respectively (Figure 3). These results suggested that Si-SeNPs exhibited an enhanced inhibitory effect on ROS production in RAW264.7 cells compared to silymarin.

3.4. The Effect of Si-SeNPs on Inflammation End Product in LPS-Induced RAW264.7 Macrophages. Several studies have confirmed that NO production, TNF-α, and IL-1β are fundamental pro-inflammatory mediators and cytokines in inflammation processes, which can lead to expression of inflammatory molecules.[19,20] As shown in Figure 4A, LPS dramatically increased the NO production to (36.1 ± 1.7 μM) compared to the untreated group (0.0 ± 0.0 μM). In contrast, treatment with Si-SeNPs remarkably reduced the LPS-induced NO secretion (15.7 ± 0.8, 9.0 ± 0.6 μM at 0.4, 0.8 μg/mL, respectively). To investigate the effects of Si-SeNPs on the cytokine secretion, an ELISA was performed in this study. In Figure 4B, TNF-α and IL-1β were slightly secreted in the untreated group; however, after 24 h of LPS stimulation, this secretion significantly increased by 209.6 and 52.9 times, respectively. Moreover, the TNF-α and IL-1β releases of the 0.8 μg/mL Si-SeNPs-treated group were markedly reduced by 47.6% and 73.0% of that in the LPS group, respectively. A slight inhibitory effect was also observed after silymarin treatment, in which the secretion of TNF-α and IL-1β was decreased by 27.1% and 37.0% compared to LPS-treated group, respectively.

To investigate whether the downregulation of TNF-α and IL-1β release was due to their gene expression induced by Si-SeNPs and silymarin, we performed a qRT-PCR analysis. The data showed that LPS caused the enhancement of TNF-α and IL-1β mRNA expression, whereas pretreatment with Si-SeNPs (0.8 μg/mL) significantly inhibited the expression of these cytokines. Additionally, compared to Si-SeNPs, pretreatment with silymarin (0.8 μg/mL) did not exhibit as effective inhibition as Si-SeNPs (Figure 4C). Consequently, these results indicated that Si-SeNPs attenuated LPS-induced NO production and pro-inflammatory cytokine expression more effectively than silymarin alone.

3.5. The Effect of Si-SeNPs on NF-κB Signaling Pathway in LPS-Stimulated RAW264.7 Cells. To examine the molecular mechanism of the inhibitory effect of Si-SeNPs on the release of pro-inflammatory cytokines from macrophages induced by LPS, western blotting was performed. In RAW264.7 cells stimulated by LPS, the relative expression of p-IκBα and p-NF-κB exhibited significant phosphorylation, whereas these phosphorylation levels were substantially decreased in the nanoparticle-treated group (Figure 5A). In addition, we further assessed whether Si-SeNPs suppress the activation of NF-κB in RAW264.7 cells by utilizing immunofluorescence staining. In comparison to the untreated group, NF-κB in the LPS stimulation group translocated and accumulated from the cytoplasm to the nucleus; however, it noticeably decreased by 51.6% and 73.4% in the 0.4 and 0.8 μg/mL Si-SeNPs groups, respectively (Figure 5B). Therefore, these results suggested that

https://doi.org/10.1021/acsomega.2c04140
ACS Omega 2022, 7, 42723−42732

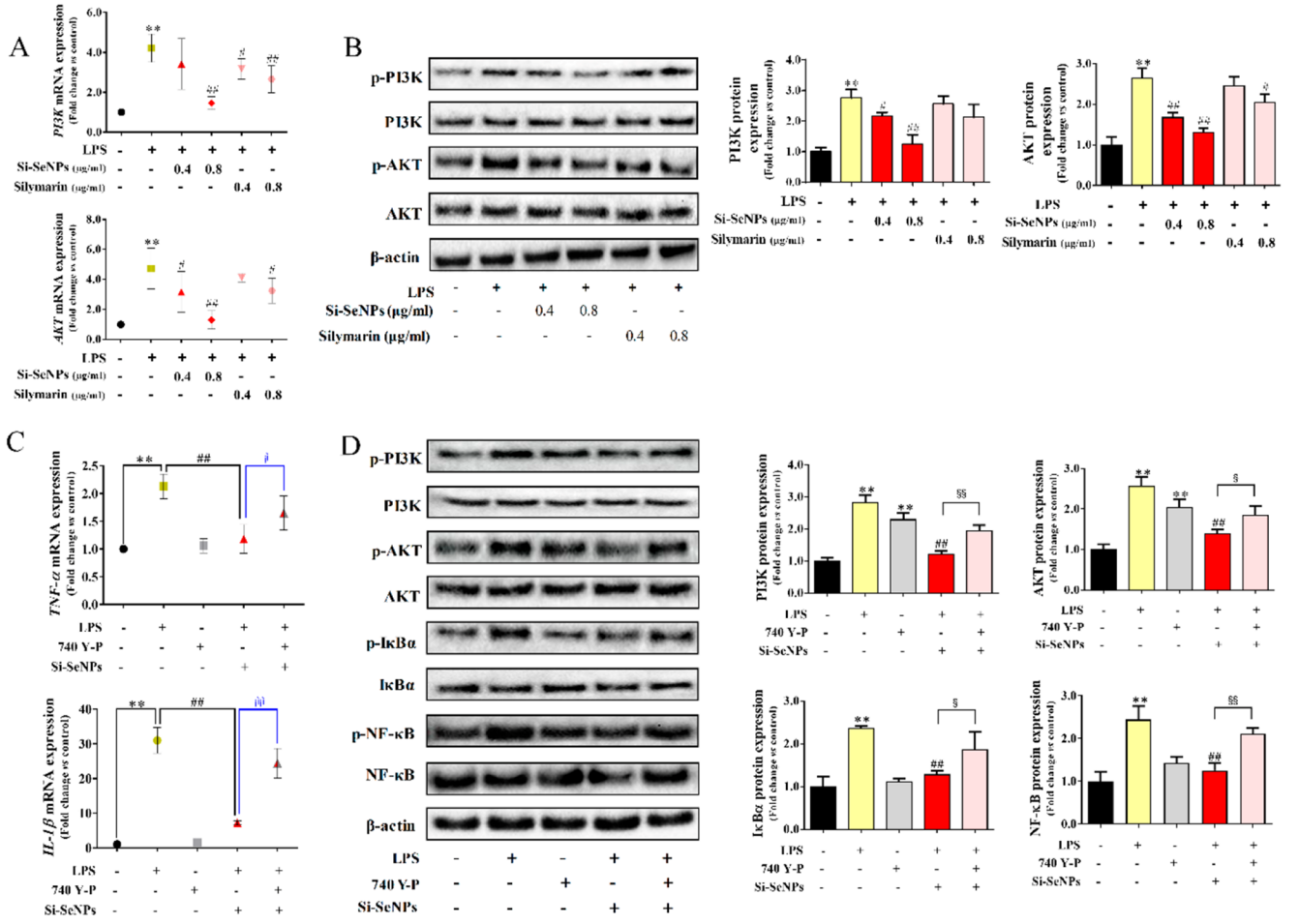

Figure 6. PI3K/Akt/NF-κB pathway is involved in Si-SeNPs activated inhibition of inflammation. qRT-PCR analysis of *PI3K* and *Akt* mRNA in activated RAW264.7 cells (A). Western blot analysis of PI3K and Akt proteins in activated RAW264.7 cells (B). Effect of 740 Y−P on mRNA expression of *TNF-α* and *IL-1β* in Si-SeNPs treated RAW264.7 cells (C). Effect of 740 Y−P on protein expression of PI3K, Akt, IκBα, and NF-κB in Si-SeNPs-treated RAW264.7 cells (D). All values are expressed as mean ± SD. (*) $p < 0.05$, (**) $p < 0.01$ vs control group; (§) $p < 0.05$, (§§) $p < 0.01$ vs Si-SeNPs group.

Si-SeNPs considerably inhibited the nuclear translocation of NF-κB in LPS-stimulated RAW264.7 macrophages.

3.6. The Inhibitory Effect of Si-SeNPs on PI3K/Akt Signaling Pathway. PI3K/Akt signaling pathway was proved to play a fundamental role at the initiation of inflammatory mechanisms.[21] Hence, we examined the PI3K/Akt pathway as an upstream signal of the anti-inflammatory mechanism of Si-SeNPs, and pretreatment with Si-SeNPs significantly inhibited PI3K and Akt expression in both gene and protein level.

To further demonstrate the biological correlation between the PI3K/Akt signaling pathway and the anti-inflammatory activity of Si-SeNPs, 740 Y−P (a PI3K activator) was used to cotreat with Si-SeNPs. As shown in Figure 6C, 740Y−P (30 μM) partially reversed TNF-α and IL-1β mRNA expression in Si-SeNPs-treated RAW264.7 cells, which confirmed that 740Y−P could inhibit the anti-inflammatory activity of Si-SeNPs. Furthermore, we investigated the protein expression that could be involved in the PI3K/Akt/NF-κB signaling cascade. As demonstrated in Figure 6D, 740 Y−P reversed the suppression of PI3K, Akt, IκBα, and NF-κB in Si-SeNPs-treated RAW264.7 cells. These data indicated that the anti-inflammatory effect of Si-SeNPs was mediated through the PI3K/Akt/NF-κB signaling pathway in RAW264.7 macrophages.

4. DISCUSSION

In recent years, an increasing number of studies have contributed more reliable evidence to the health-promoting properties of SeNPs. However, traditional physical and chemical synthesis methods of SeNPs require hazardous elements and extreme thermal conditions, which are perilous for biological applications.[22] Beyond the benefits of a biological synthesis of SeNPs such as environmental friendliness and unique spectroscopic characteristics, natural plant-mediated biological synthesis of SeNPs is known to be a less toxic, easier, and more cost-effective approach, having been proven to have the ability to perform as reducing and capping agents.[15] Rad et al. fabricated SeNPs using *Pelargonium zonale* leaf extract for enhanced antimicrobial activities.[23] Qiu et al. reported that pectin-decorated SeNPs exhibited stability and enhanced antioxidant activity.[24] In our previous study, silymarin-mediated SeNPs were successfully synthesized in an eco-friendly, efficient, economical, and more suitable for biological applications manner.

TEM, energy-dispersive X-ray spectrometry (EDX), and Fourier transform infrared spectroscopy (FTIR) were used to confirm the formation of Si-SeNPs, with sizes ranging from 30 to 80 nm and mixed shape.[8] Interestingly, in this study, the

https://doi.org/10.1021/acsomega.2c04140
ACS Omega 2022, 7, 42723−42732

hydrodynamic size of Si-SeNPs substantially increased compared to the TEM result, which was confirmed by the DLS measurement. An acceptable explanation for this change is that DLS takes the organic shell of the SeNPs into consideration and measures the total size of the conjugate in colloids. The number of biomolecules covering each SeNP was huge; therefore, the hydrodynamic size measured using DLS was greater than that measured by TEM.[25] In addition, the zeta potential value of Si-SeNPs was −32.2 mV, which might be derived from the benefit of loading silymarin as a capping agent and stabilizer, suggesting its high stability. Being consistent with our results, Rajkumar et al. indicated that SeNPs synthesized using banana peel extract had higher stability capacity than SeNPs synthesized using commercial media.[26] To corroborate the advantages of Si-SeNPs as a vector for drugs, the anti-inflammatory activities of synthesis Si-SeNPs were studied in LPS-stimulated RAW264.7 cells in the present study, compared to solely silymarin extract.

Macrophages are an important host defense against the pathogenesis of many infectious, immunological, and degenerative disease processes.[27] After stimulation with LPS, various pro-inflammatory cytokines and mediators are released by macrophages, including NO, TNF-α, and IL-1β. Excessive secretion would cause extensive tissue damage and pathological changes.[28] Wang et al. reported that SeNPs could considerably decrease NO production in RAW264.7 cells.[29] Similar to this result, although silymarin showed only a slight inhibitory effect, Si-SeNPs exhibited significantly enhanced inhibition on LPS-stimulated NO production. TNF-α and IL-1β are known to be the predominant pro-inflammatory cytokines released by LPS.[30] In particular, their essential role in cell proliferation and differentiation is the induced expression of proteins associated with acute inflammation.[31] Our results showed that Si-SeNPs strongly suppressed TNF-α and IL-1β secretion in RAW264.7 macrophages. In addition, the inhibitory effect of Si-SeNPs (0.8 μg/mL) on those cytokines was 20.5% and 36.8% higher than that of silymarin (0.8 μg/mL), respectively. Therefore, the effective inhibition of LPS-induced cytokine production by Si-SeNPs may be due to the synergistic effect of silymarin and SeNPs.

The mechanism by which Si-SeNPs might suppress LPS-activated inflammatory signaling pathways was explored. The NF-κB signaling pathway serves as the regulator of inflammatory responses, taking responsibility for mediating the induction of various pro-inflammatory genes including encoding cytokines in macrophages.[32] When macrophages are challenged with LPS, IκBα will be activated, resulting in the ubiquitination and degradation; consequently, NF-κB translocates to the nucleus, leading to the induction of target genes.[33] In our study, we concluded that a Si-SeNPs pretreatment significantly suppressed the LPS-induced phosphorylation of IκBα and NF-κB in RAW264.7 macrophages. Immunofluorescence images suggested that Si-SeNPs were able to inhibit the translocation of phosphorylated p65 to the nucleus. Our present findings are in accordance with a previous investigation of Wang et al. that demonstrated the SeNPs decorated with a *Ganoderma lucidum* polysaccharide exhibited anti-inflammatory activity by inhibiting the NF-κB pathway.[29] Zhu et al. reported that SeNPs coated with *Ulva lactuca* polysaccharide suppressed the nuclear translocation of NF-κB, thereby offering the therapeutic potential for reducing the symptoms of acute colitis.[34]

Numerous researchers have demonstrated that the PI3K/Akt signaling pathway has a function as an upstream activator of the NF-κB signaling cascade, causing phosphorylation of NF-κB and IκBα, which further leads to the release of inflammatory constituents and cell damage.[35,36] Therefore, we explored the effect of Si-SeNPs on PI3K/Akt signaling in LPS-induced RAW264.7 cells. Western blotting results reported that Si-SeNPs significantly inhibited LPS-induced phosphorylation of PI3K and Akt. To verify whether Si-SeNPs could play a functional role in attenuating the PI3K/Akt/NF-κB signaling pathway, we pretreated RAW264.7 cells with 740 Y−P and found that 740 Y−P could partially reverse the inhibitory effects of Si-SeNPs on the NF-κB cascade and pro-inflammatory cytokines, supporting a causal role for the PI3K/Akt signaling pathway in the anti-inflammatory effect of Si-SeNPs. These results implied that Si-SeNPs reduced LPS-induced inflammatory responses by downregulating the PI3K/Akt-mediated NF-κB signaling pathway.

5. CONCLUSIONS

In conclusion, the present study has developed a green technique for synthesizing silymarin-mediated SeNPs and investigated its anti-inflammatory activities in RAW264.7 macrophages. Particularly, Si-SeNPs significantly decreased the level of ROS release and NO production by 83.3% and 75.0%, respectively. Furthermore, our investigation indicated that Si-SeNPs exhibit greater anti-inflammatory activities toward RAW264.7 cells compared to silymarin. Although further studies are required to corroborate the molecular mechanism in RAW264.7 cells, our findings presented that Si-SeNPs suppressed LPS-induced NF-κB activation by potentially downregulating the PI3K/Akt signaling pathway, which further inhibits the release of pro-inflammatory cytokines and mediators. These findings suggest that Si-SeNPs are a promising agent with anti-inflammatory activity in vitro. In brief, these results could be valuable for the development of biosynthesized SeNPs and their use as novel candidates in inflammatory diseases.

AUTHOR INFORMATION

Corresponding Author

Yeon-Ju Kim − *Graduate School of Biotechnology, and College of Life Science, Kyung Hee University, Yongin-si 17104 Gyeonggi-do, Republic of Korea;* orcid.org/0000-0002-3474-066X; Phone: +82-31-201-2645; Email: yeonjukim@khu.ac.kr; Fax: +82-31-204-8116

Authors

Xiao-jie Mi − *Graduate School of Biotechnology, and College of Life Science, Kyung Hee University, Yongin-si 17104 Gyeonggi-do, Republic of Korea*

Ha-Minh Le − *Graduate School of Biotechnology, and College of Life Science, Kyung Hee University, Yongin-si 17104 Gyeonggi-do, Republic of Korea*

Sanghyun Lee − *Department of Plant Science and Technology, Chung Ang University, Anseong 17546, Republic of Korea*

Hye-Ryung Park − *Graduate School of Biotechnology, and College of Life Science, Kyung Hee University, Yongin-si 17104 Gyeonggi-do, Republic of Korea*

Complete contact information is available at: https://pubs.acs.org/10.1021/acsomega.2c04140

Author Contributions

[§]These authors contributed equally to this work.

https://doi.org/10.1021/acsomega.2c04140
ACS Omega 2022, 7, 42723−42732

Notes

The authors declare no competing financial interest.

■ ACKNOWLEDGMENTS

This work was supported by a grant from the Basic Science Research Program through the National Research Foundation of Korea funded by the Ministry of Education (Grant No. 2019R1A2C1010428);the Natural Product Institute of Science and Technology (Anseong, Republic of Korea).

■ REFERENCES

(1) Chen, L.; Deng, H.; Cui, H.; Fang, J.; Zuo, Z.; Deng, J.; Li, Y.; Wang, X.; Zhao, L. Inflammatory responses and inflammation-associated diseases in organs. *Oncotarget* **2018**, *9* (6), 7204−7218.

(2) Zhou, Y.; Wang, J.; Yang, W.; Qi, X.; Lan, L.; Luo, L.; Yin, Z. Bergapten prevents lipopolysaccharide-induced inflammation in RAW264.7 cells through suppressing JAK/STAT activation and ROS production and increases the survival rate of mice after LPS challenge. *Int. Immunopharmacol* **2017**, *48*, 159−168.

(3) Oishi, Y.; Manabe, I. Macrophages in inflammation, repair and regeneration. *Int. Immunol.* **2018**, *30* (11), 511−528.

(4) Azab, A.; Nassar, A.; Azab, A. N. Anti-inflammatory activity of natural products. *Molecules* **2016**, *21* (10), 1321.

(5) Behrens, E. M.; Koretzky, G. A. Review: Cytokine storm syndrome: Looking toward the precision medicine era. *Arthritis Rheumatol* **2017**, *69* (6), 1135−1143.

(6) Varga, Z.; Sabzwari, S. R. A.; Vargova, V. Cardiovascular risk of nonsteroidal anti-inflammatory drugs: An under-recognized public health issue. *Cureus* **2017**, *9* (4), No. e1144.

(7) Di Costanzo, A.; Angelico, R. Formulation strategies for enhancing the bioavailability of silymarin: the state of the art. *Molecules* **2019**, *24* (11), 2155.

(8) Mi, X. J.; Choi, H. S.; Perumalsamy, H.; Shanmugam, R.; Thangavelu, L.; Balusamy, S. R.; Kim, Y. J. Biosynthesis and cytotoxic effect of silymarin-functionalized selenium nanoparticles induced autophagy mediated cellular apoptosis via downregulation of PI3K/Akt/mTOR pathway in gastric cancer. *Phytomedicine* **2022**, *99*, 154014.

(9) Kim, J.; Paje, L. A.; Choi, J. W.; Lee, H.-D.; Shim, J. S.; Shim, J.; Geraldino, P. J. L.; Lee, S. Determination of silymarin and silybin diastereomers in Korean milk thistle using HPLC/UV analysis. *Korean J. Pharmacognosy* **2020**, *51* (4), 297−301.

(10) Zamani-Garmsiri, F.; Emamgholipour, S.; Rahmani Fard, S.; Ghasempour, G.; Jahangard Ahvazi, R.; Meshkani, R. Polyphenols: Potential anti-inflammatory agents for treatment of metabolic disorders. *Phytother Res.* **2022**, *36* (1), 415−432.

(11) Patra, J. K.; Das, G.; Fraceto, L. F.; Campos, E. V. R.; Rodriguez-Torres, M. d. P.; Acosta-Torres, L. S.; Diaz-Torres, L. A.; Grillo, R.; Swamy, M. K.; Sharma, S.; Habtemariam, S.; Shin, H.-S. Nano based drug delivery systems: recent developments and future prospects. *J. Nanobiotechnol* **2018**, *16* (1), 71.

(12) Wang, H.; Xu, M. Z.; Liang, X. Y.; Nag, A.; Zeng, Q. Z.; Yuan, Y. Fabrication of food grade zein-dispersed selenium dual-nanoparticles with controllable size, cell friendliness and oral bioavailability. *Food Chem.* **2023**, *398*, 133878−133884.

(13) Ferro, C.; Florindo, H. F.; Santos, H. A. Selenium nanoparticles for biomedical applications: From development and characterization to therapeutics. *Adv. Healthc Mater.* **2021**, *10* (16), No. 2100598.

(14) Andra, S.; Balu, S. K.; Jeevanandham, J.; Muthalagu, M.; Vidyavathy, M.; Chan, Y. S.; Danquah, M. K. Phytosynthesized metal oxide nanoparticles for pharmaceutical applications. *Naunyn Schmiedebergs Arch Pharmacol* **2019**, *392* (7), 755−771.

(15) Skalickova, S.; Milosavljevic, V.; Cihalova, K.; Horky, P.; Richtera, L.; Adam, V. Selenium nanoparticles as a nutritional supplement. *Nutrition* **2017**, *33*, 83−90.

(16) Yeung, Y. T.; Aziz, F.; Guerrero-Castilla, A.; Arguelles, S. Signaling pathways in inflammation and anti-inflammatory therapies. *Curr. Pharm. Design* **2018**, *24* (14), 1449−1484.

(17) Soleimani, V.; Delghandi, P. S.; Moallem, S. A.; Karimi, G. Safety and toxicity of silymarin, the major constituent of milk thistle extract: An updated review. *Phytother Res.* **2019**, *33* (6), 1627−1638.

(18) Zhang, Y.; Choksi, S.; Chen, K.; Pobezinskaya, Y.; Linnoila, I.; Liu, Z. G. ROS play a critical role in the differentiation of alternatively activated macrophages and the occurrence of tumor-associated macrophages. *Cell Res.* **2013**, *23* (7), 898−914.

(19) Wojdasiewicz, P.; Poniatowski, L. A.; Szukiewicz, D. The role of inflammatory and anti-inflammatory cytokines in the pathogenesis of osteoarthritis. *Mediators Inflamm* **2014**, *2014*, 561459.

(20) Sharma, J. N.; Al-Omran, A.; Parvathy, S. S. Role of nitric oxide in inflammatory diseases. *Inflammopharmacology* **2007**, *15* (6), 252−9.

(21) He, L.; Pan, Y.; Yu, J.; Wang, B.; Dai, G.; Ying, X. Decursin alleviates the aggravation of osteoarthritis via inhibiting PI3K-Akt and NF-kB signal pathway. *Int. Immunopharmacol* **2021**, *97*, 107657.

(22) Iranifam, M.; Fathinia, M.; Sadeghi Rad, T.; Hanifehpour, Y.; Khataee, A. R.; Joo, S. W. A novel selenium nanoparticles-enhanced chemiluminescence system for determination of dinitrobutylphenol. *Talanta* **2013**, *107*, 263−9.

(23) Rad, S. S.; Sani, A. M.; Mohseni, S. Biosynthesis, characterization and antimicrobial activities of zinc oxide nanoparticles from leaf extract of Mentha pulegium (L.). *Microb Pathog* **2019**, *131*, 239−245.

(24) Qiu, W. Y.; Wang, Y. Y.; Wang, M.; Yan, J. K. Construction, stability, and enhanced antioxidant activity of pectin-decorated selenium nanoparticles. *Colloid Surface B* **2018**, *170*, 692−700.

(25) Boroumand, S.; Safari, M.; Shaabani, E.; Shirzad, M.; Faridi-Majidi, R. Selenium nanoparticles: synthesis, characterization and study of their cytotoxicity, antioxidant and antibacterial activity. *Mater. Res. Express* **2019**, *6*, 0850d8.

(26) Rajkumar, K.; MVS, S.; Koganti, S.; Burgula, S. Selenium nanoparticles synthesized using pseudomonas stutzeri (MH191156) show antiproliferative and anti-angiogenic activity against cervical cancer cells. *Int. J. Nanomed.* **2020**, *15*, 4523−4540.

(27) Liu, Y.; Perumalsamy, H.; Kang, C. H.; Kim, S. H.; Hwang, J. S.; Koh, S. C.; Yi, T. H.; Kim, Y. J. Intracellular synthesis of gold nanoparticles by Gluconacetobacter liquefaciens for delivery of peptide CopA3 and ginsenoside and anti-inflammatory effect on lipopolysaccharide-activated macrophages. *Artif Cell Nanomed B* **2020**, *48* (1), 777−788.

(28) Guo, M.; Xiao, J.; Sheng, X.; Zhang, X.; Tie, Y.; Wang, L.; Zhao, L.; Ji, X. Ginsenoside Rg3 mitigates atherosclerosis progression in diabetic apoE−/− mice by skewing macrophages to the M2 phenotype. *Front. Pharmacol.* **2018**, *9*, 464.

(29) Wang, J.; Zhang, Y.; Yuan, Y.; Yue, T. Immunomodulatory of selenium nano-particles decorated by sulfated Ganoderma lucidum polysaccharides. *Food Chem. Toxicol.* **2014**, *68*, 183−9.

(30) Park, J. Y.; Chung, T. W.; Jeong, Y. J.; Kwak, C. H.; Ha, S. H.; Kwon, K. M.; Abekura, F.; Cho, S. H.; Lee, Y. C.; Ha, K. T.; Magae, J.; Chang, Y. C.; Kim, C. H. Ascofuranone inhibits lipopolysaccharide-induced inflammatory response via NF-κB and AP-1, p-ERK, TNF-alpha, IL-6 and IL-1beta in RAW 264.7 macrophages. *PLoS One* **2017**, *12* (2), No. e0171322.

(31) Batra, R.; Suh, M. K.; Carson, J. S.; Dale, M. A.; Meisinger, T. M.; Fitzgerald, M.; Opperman, P. J.; Luo, J.; Pipinos, I. I.; Xiong, W.; Baxter, B. T. IL-1beta (Interleukin-1beta) and TNF-alpha (Tumor Necrosis Factor-alpha) impact abdominal aortic aneurysm formation by differential effects on macrophage polarization. *Arterioscler Thromb Vasc Biol.* **2018**, *38* (2), 457−463.

(32) Yu, H.; Lin, L.; Zhang, Z.; Zhang, H.; Hu, H. Targeting NF-κB pathway for the therapy of diseases: mechanism and clinical study. *Signal Transduct Target Ther* **2020**, *5* (1), 209.

(33) Mann, M.; Mehta, A.; Zhao, J. L.; Lee, K.; Marinov, G. K.; Garcia-Flores, Y.; Lu, L. F.; Rudensky, A. Y.; Baltimore, D. An NF-κB-microRNA regulatory network tunes macrophage inflammatory responses. *Nat. Commun.* **2017**, *8* (1), 851.

(34) Zhu, C. H.; Zhang, S. M.; Song, C. W.; Zhang, Y. B.; Ling, Q. J.; Hoffmann, P. R.; Li, J.; Chen, T. F.; Zheng, W. J.; Huang, Z. Selenium nanoparticles decorated with Ulva lactuca polysaccharide potentially

https://doi.org/10.1021/acsomega.2c04140
ACS Omega 2022, 7, 42723−42732

attenuate colitis by inhibiting NF-κB mediated hyper inflammation. *J. Nanobiotechnol.* **2017**, *15* (1), 20.
(35) Ngabire, D.; Seong, Y. A.; Patil, M. P.; Niyonizigiye, I.; Seo, Y. B.; Kim, G. D. Anti-inflammatory effects of aster incisus through the inhibition of NF-κB, MAPK, and Akt pathways in LPS-stimulated RAW 264.7 macrophages. *Mediat Inflamm* **2018**, *2018*, 4675204.
(36) Li, W.; Du, Q.; Li, X.; Zheng, X.; Lv, F.; Xi, X.; Huang, G.; Yang, J.; Liu, S. Eriodictyol inhibits proliferation, metastasis and induces apoptosis of glioma cells via PI3K/Akt/NF-κB signaling pathway. *Front Pharmacol* **2020**, *11*, 114.

https://doi.org/10.1021/acsomega.2c04140
ACS Omega 2022, 7, 42723−42732